

Copy 298

RM A55L06

NACA RM A55L06



Reg H 14705
12-1956

0143354



TECH LIBRARY KAFB, NM

RESEARCH MEMORANDUM

A SIMULATION STUDY OF A WINGLESS MISSILE

By Henry C. Lessing and David E. Reese, Jr.

Ames Aeronautical Laboratory
Moffett Field, Calif.

HADC
TECHNICAL LIBRARY
AFL 2811

CLASSIFIED DOCUMENT

This material contains information affecting the National Defense of the United States within the meaning of the espionage laws, Title 18, U.S.C., Secs. 793 and 794, the transmission or revelation of which in any manner to an unauthorized person is prohibited by law.

NATIONAL ADVISORY COMMITTEE
FOR AERONAUTICS

WASHINGTON

February 8, 1956



Moss Unclassified
By ~~Mr.~~ NASA Tech Pub Announcement #4
13, 16 Mar. 59

GRADE OF OFFICER MAKING CHANGE) NK
DATE 14 Mar. 61



NATIONAL ADVISORY COMMITTEE FOR AERONAUTICS

RESEARCH MEMORANDUM

A SIMULATION STUDY OF A WINGLESS MISSILE

By Henry C. Lessing and David E. Reese, Jr.

SUMMARY

A preliminary study to determine the possibility of utilizing a wingless configuration as a guided missile has been made. The steady-state lift and drag characteristics and the results of a simulation study to determine the missile's tracking performance when utilized as a beam rider are presented. In order to establish a frame of reference with which to evaluate the performance of the wingless configuration, results are also presented for a conventional winged, cruciform missile.

The results of the investigation indicate that the maximum trimmed lift coefficient developed by the wingless missile was somewhat smaller than that of the winged missile at a Mach number of 2.4. The data also show that, at the higher Mach numbers, the drag coefficient of the wingless missile will be somewhat greater than that of the cruciform missile both at the zero and maximum trimmed lift conditions, due to the high drag of the control and stabilizing surfaces. However, the tracking capabilities of the wingless missile as determined from the simulation study compare favorably with the cruciform missile at the Mach numbers investigated.

INTRODUCTION

The guided antiaircraft missile as an operational weapon is a fairly recent development. The design of currently operational missiles was initiated approximately ten years ago and proceeded as a conservative guess because of the lack of previous experience and suitable data. The result has been that every missile to date has incorporated sizable lifting surfaces, usually of cruciform arrangement.

The use of large lifting surfaces has presented one of the difficulties in the integration of the missile and the fighter aircraft as an effective weapon system; that is, the additional drag associated with missile stowage resulting in a loss in performance. Efforts are now being made to reduce this performance penalty imposed on missile-carrying fighter aircraft. Reference 1 presents the results of a study which compares the tracking capabilities of a cruciform missile and a monowing missile for which the additional drag should be reduced. The obvious

extension of this trend would be the possible use of a wingless missile. The purpose of the present report is to present the results of a preliminary study made to determine the feasibility of utilizing such a wingless configuration as a guided missile.

SYMBOLS

a_z	normal acceleration, ft/sec ²
c_c	axial-force coefficient, $\frac{\text{axial force}}{q_0 S}$
c_d	drag coefficient, $\frac{\text{drag}}{q_0 S}$
c_l	rolling-moment coefficient about body longitudinal axis, $\frac{\text{rolling moment}}{q S d}$
c_L	lift coefficient, $\frac{\text{lift}}{q_0 S}$
c_m	pitching-moment coefficient, $\frac{\text{pitching moment}}{q_0 S d}$
c_N	normal-force coefficient, $\frac{\text{normal force}}{q_0 S}$
d	body diameter, ft
g	acceleration due to gravity, ft/sec ²
I_x, I_y, I_z	roll, pitch, and yaw moments of inertia about center of gravity, slug-ft ²
M	free-stream Mach number
m	missile mass, slugs
q_0	free-stream dynamic pressure, lb/ft ²
q	pitching velocity, radians/sec
S	maximum cross-sectional area of body, ft ²

CONFIDENTIAL

α	angle of attack of body longitudinal axis, deg
β	angle of sideslip of body longitudinal axis, deg
δ_p, δ_y	pitch, yaw control deflection measured with respect to surface of nose cone, deg
φ	roll angle, radians

WINGLESS MISSILE CHARACTERISTICS

Wind-tunnel studies of several wingless missiles have been made (e.g., refs. 2 and 3). The particular missile and mass characteristics selected for the present study are shown in figure 1(a). The missile stabilizing surfaces were formed by four segments of the body which projected laterally into the air stream at a deflection angle of 20° . The flat sides of the deflected segments were intended to simulate their extension by means of bellows after the missile had been fired. The control surfaces consisted of four flaps which, when retracted, formed a portion of the external contour of the nose. The maximum deflection of the control surfaces was 30° measured with respect to the surface of the conical nose.

The longitudinal aerodynamic characteristics of the wingless missile are presented in figure 2 for Mach numbers of 2.44 and 3.35. These data were obtained in one of the Ames 1- by 3-foot supersonic wind tunnels at a Reynolds number of 8 million per foot. The axial force on the base of the model, determined from measured base pressures and free-stream static pressures, were subtracted from measured total forces; thus, the axial force data presented correspond to a base pressure equal to free-stream static pressure.

Examination of the wingless missile will show that rolling moments are produced primarily by a combination of an angle of attack with a yaw control deflection or an angle of yaw with a pitch control deflection. The rolling-moment coefficient generated by the nose control at a Mach number of 2.2 is shown in figure 3. These data were obtained for the nose section only and at a Mach number different than that of the foregoing data because of the unavailability of suitable testing facilities at the time of the investigation. The facility used was the Ames 8- by 8-inch wind tunnel. The Reynolds number of the test was 15 million per foot. These data show that the rolling moments are very small and, although these results were obtained only for the conical-nose section of the missile, it is felt that the rolling moments for the complete configuration will not differ greatly from those shown, due primarily to low lift effectiveness of the type of stabilizing surfaces used.

WINGLESS MISSILE EVALUATION

The criteria used to evaluate the performance of the wingless missile were the maximum trimmed-lift coefficient, the drag coefficient at zero lift and at maximum trimmed-lift coefficient, and the tracking capability when used as a beam-rider missile. In order to make the results as meaningful as possible, the performance of the variable-incidence cruciform-winged missile shown in figure 1(b) was chosen as a frame of reference for the evaluation. Wind-tunnel and flight-test data pertaining to this missile are available (e.g., refs. 4 and 5) from which the lift and drag characteristics may be obtained. In addition, the tracking capabilities of the missile at a Mach number of 1.5 have been investigated (ref. 1) and were available for use in this part of the evaluation.

It will be noted in the discussion to follow that the data for the two missiles are presented for different Mach number ranges. As stated above, the data for the cruciform missile were obtained from existing wind-tunnel and flight-test investigations and the Mach number range of these investigations represents the range over which the missile was intended to perform adequately. The tactical requirements for missiles have changed since the design of the cruciform missile, however, and a higher speed range is desirable. For this reason, the wingless missile was investigated over a somewhat higher Mach number range than that for the cruciform missile.

It was necessary to select a center-of-gravity position for the evaluation of the wingless missile. (The location of the center of gravity for the cruciform missile was established in previous papers concerned with this missile.) It was recognized, of course, that both the maximum trimmed-lift coefficient and the stability of the missile would be functions of the center-of-gravity location and that some sort of compromise between high trimmed-lift capability and adequate stability would have to be made. The particular center-of-gravity location selected for this study was 52.8 percent of the body length aft of the nose and is shown in figure 1(a). The center-of-gravity location for the cruciform missile was 49.7 percent of the body length aft of the nose and is shown in figure 1(b).

Lift Effectiveness

The maximum trimmed-lift coefficients for the wingless and the cruciform missiles as a function of Mach number are shown in figure 4. The two curves for the cruciform missile represent the normal and lateral trimmed-lift coefficients as determined by control deflections in pitch and yaw of 17° and 13° , respectively. The control deflections were

CONFIDENTIAL

limited to these values by mechanical interference between wing panels. The coefficients for both missiles are based on body cross-sectional area.

It can be seen that at the higher Mach numbers the trimmed-lift coefficient of the cruciform missile begins to approach that for the wingless missile. Although the maximum trimmed-lift coefficient of the wingless missile is lower than that for the cruciform arrangement, further study is necessary to determine if such a decrease in lift capability is acceptable. A partial answer to this question is provided by the results of the simulation study which will be discussed later.

Also noted in figure 4 are the angles of attack necessary to obtain the indicated lift coefficients for the two missiles. The maximum trimmed angle of attack of the wingless missile is larger than that for the variable incidence cruciform missile and, although this characteristic should present no difficulties in the case of a beam-rider missile, its effect on other types of guidance must be investigated.

Drag

The drag coefficient at zero lift and at maximum trimmed lift is shown in figure 5 as a function of Mach number for the two missiles. The drag coefficient of the wingless missile is somewhat greater than that of the cruciform missile both at zero and maximum lift, due to the high drag characteristics of the control and stabilizing surfaces. A significant reduction in drag can be obtained through the use of a single set of surfaces for both stabilization and control. Unpublished calculations indicate that if the surfaces of the type used for stabilization on the present missile are also used for control, appreciable reduction of the drag may be realized without a reduction in control effectiveness. Research is continuing on this phase of the problem.

Simulation Study

The simulation problem studied was the same as that presented in reference 1, an investigation of the performance of the missile while tracking a maneuvering target with glint noise present. The study was conducted on a Reeves Electronic Analog Computer. Five degrees of freedom were considered, the sixth, forward velocity, being assumed constant for the duration of the tracking run.

It was necessary to make certain assumptions and approximations in order to introduce the aerodynamic characteristics of the wingless missile into the computing equipment for the simulation study. The non-linear aerodynamic characteristics of the wingless missile shown in

CONFIDENTIAL

figures 2 and 3 were approximated by polynomial expressions. The normal-force coefficient contributed by control deflection is seen from figure 2 to be very small and was neglected. In addition, the effect of Mach number on normal force is negligible, hence a single expression relating the normal-force coefficient to angle of attack was used in the simulation for both Mach numbers. The pitching-moment curves were approximated in the study by fitting the 0° and 30° control-deflection curves with polynomial expressions and interpolating for the curves corresponding to intermediate deflections approximately as the square of δ . Different polynomials were used for each of the two Mach numbers. While some smoothing of the data resulted at a Mach number of 2.44, excellent reproduction of the data was possible at a Mach number of 3.35. Although the rolling-moment data of figure 3 were obtained at a Mach number other than that of the rest of the data, it was felt that Mach number effects would be minor and, consequently, these data were used in the simulation study. Unstable pitching and yawing moments are produced by a yaw control deflection when at angle of attack and a pitch control deflection when at angle of yaw. As no experimental data were available, these quantities were estimated from the rolling-moment data. No interference effects between the control and stabilizing surfaces were included in these calculations, and it is not known what effects will actually be present. Because of the extremely small values of the damping in pitch and roll of the wingless missile, these quantities were assumed to be zero. Although it is anticipated that removal of the main lifting surfaces could result in an appreciable reduction in weight, and a subsequent increase in maneuverability, the mass characteristics of the wingless missile were assumed identical to those of the cruciform missile with the exception of the roll moment of inertia which was reduced by an amount equal to that for the four wing panels.

The beam-rider geometry is shown in figure 6. The illustration represents a tail chase of a target accelerating laterally, with the plane of the figure being perpendicular to the beam. The position of the beam is determined by the tracking radar of the interceptor, the difference between the beam and the target positions being caused primarily by glint noise. A free gyroscope in the missile measures the roll angle and resolves the error into missile coordinates.

A block diagram of the control system of the wingless missile is shown in figure 7. Only the pitch system is shown in the figure as the yaw system was identical in every respect. The components of the system are essentially those of the cruciform missile studied in reference 1 with the exception that the altitude and Mach number gain changer has been removed. The roll control system, whose primary function is to limit rolling velocities, was eliminated also as there were no specific roll control surfaces on the wingless missile. The two quantities V_p and V_y represent voltages proportional to the resolved missile-beam errors shown in figure 6. These voltages drive the pitch and yaw control systems to produce acceleration of the missile in the desired direction.

In reference 1 the maximum control deflections of the cruciform missile in pitch and in yaw were assumed to be 17° , and the missile was not allowed to roll. It is this somewhat idealized version of the cruciform missile that will be used to evaluate the tracking capabilities of the wingless missile.

Time histories of the beam inputs to the missile control systems are shown in figure 8. The effect of the glint noise was simulated by using an actual 14-second radar tracking record taken during a tail chase of a nonmaneuvering F6F airplane. The root-mean-square miss distance of this noise record is approximately 18 feet. The target motion was assumed to be an alternating $1.5g$ lateral acceleration.

The beam-riding qualities of the wingless missile were investigated for Mach numbers of 2.44 and 3.35 for an altitude of 50,000 feet. The results of the tracking run at a Mach number of 3.35 can be seen in figure 9. The peak angles of attack and sideslip obtained were of the order of 20° to 25° . Corresponding to these angles, peak values of normal and lateral accelerations of approximately $20g$'s were developed. As mentioned earlier, the rolling moments were very small and produced relatively low values of roll velocity, even though the damping in roll was assumed to be zero. As shown, the rolling velocity reaches a peak value of approximately 13 radians per second and thereafter returns to essentially zero. Examination of the miss distances occurring during the 14-second tracking run shows that peak values of approximately 45 feet were reached. If, as in reference 1, the missile is assumed to be constantly at intercept, then a measure of the tracking capability is the root-mean-square error for the entire run. The tracking results for the two missiles at an altitude of 50,000 feet are shown in the following table:

Missile	Control deflection limits	M	RMS miss distance, ft
Cruciform	$(\delta_p, \delta_y) \leq 17^\circ$	1.5	33
Wingless	$(\delta_p, \delta_y) \leq 30^\circ$	2.44	30
		3.35	26

It should be recalled that the rms miss distance of the noise record was approximately 18 feet. At both Mach numbers the tracking capability of the wingless missile compares favorably with the cruciform missile.

CONCLUDING REMARKS

A preliminary study to determine the feasibility of utilizing a wingless configuration as a guided missile has been made. The

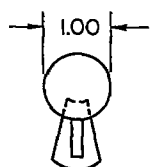
steady-state lift and drag characteristics, and the tracking capabilities when used as a beam-rider type of missile have been examined and evaluated on the basis of the performance of a conventional winged, cruciform missile. It was found that for the particular center-of-gravity location chosen the maximum trimmed-lift coefficient developed by the wingless missile was somewhat smaller than that of the winged missile at a Mach number of 2.4. In addition the data studied indicate that, at the higher Mach numbers, the drag coefficient will be somewhat greater than that of the cruciform missile both at the zero and maximum trimmed-lift conditions due to the high drag of the stabilizing and control surfaces. The tracking capabilities of the wingless missile as determined from the simulation study compare favorably with the cruciform missile at the Mach numbers investigated.

Ames Aeronautical Laboratory
National Advisory Committee for Aeronautics
Moffett Field, Calif., Dec. 6, 1955

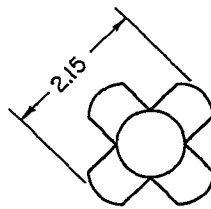
REFERENCES

1. Matthews, Howard F., and Schmidt, Stanley F.: A Comparison of the Maneuvering Performance of a Monowing Versus a Cruciform Missile. NACA RM A55D13, 1955.
2. Lazzeroni, Frank A.: Investigation of a Missile Airframe With Control Surfaces Consisting of Projecting Quadrants of the Nose Cone. NACA RM A53L21, 1954.
3. Eggers, A. J., Jr., and Syvertson, Clarence A.: Experimental Investigation of a Body Flare for Obtaining Pitch Stability and a Body Flap for Obtaining Pitch Control in Hypersonic Flight. NACA RM A54J13, 1955.
4. Anon.: Normal Force and Pitching Stability and Control Characteristics for Sparrow 15-C and 15-D Configurations. Rep. MTM-343, Douglas Aircraft Company, Aug. 9, 1951.
5. Delameter, H. D., Buell, D. R., and Mixon, M. S.: Summary of XAAM-N-2 Sparrow Missile Performance and Stability and Control Characteristics. Rep. No. SM-13907, Douglas Aircraft Company, Oct. 29, 1951.

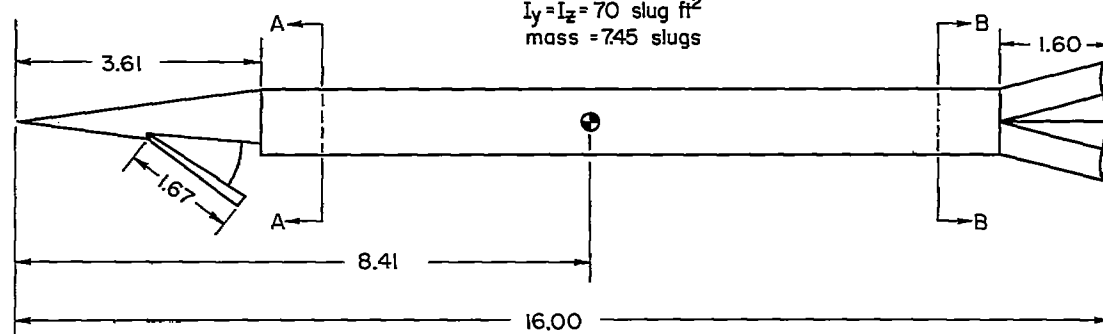
CONFIDENTIAL

~~CONFIDENTIAL~~

Section A-A

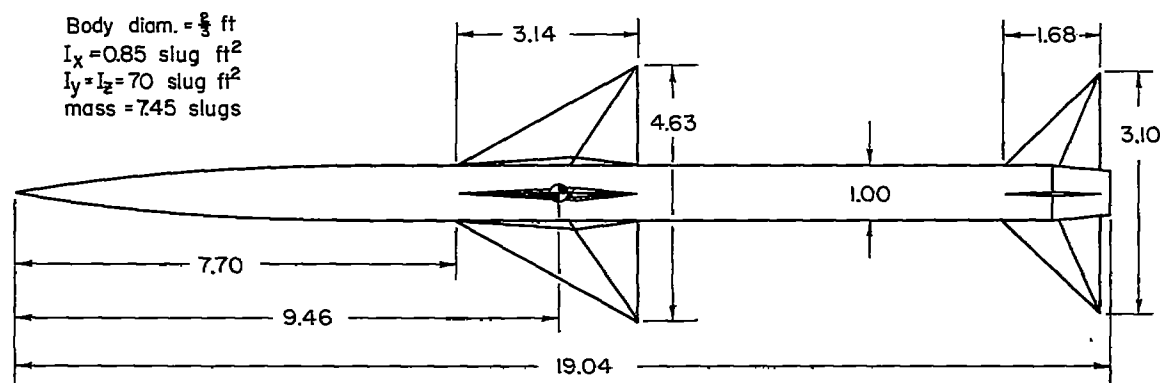


Section B-B



(a) Wingless missile.

All dimensions in terms of body diameters.



(b) Cruciform missile.

Figure 1.- Sketch of missiles.

~~CONFIDENTIAL~~

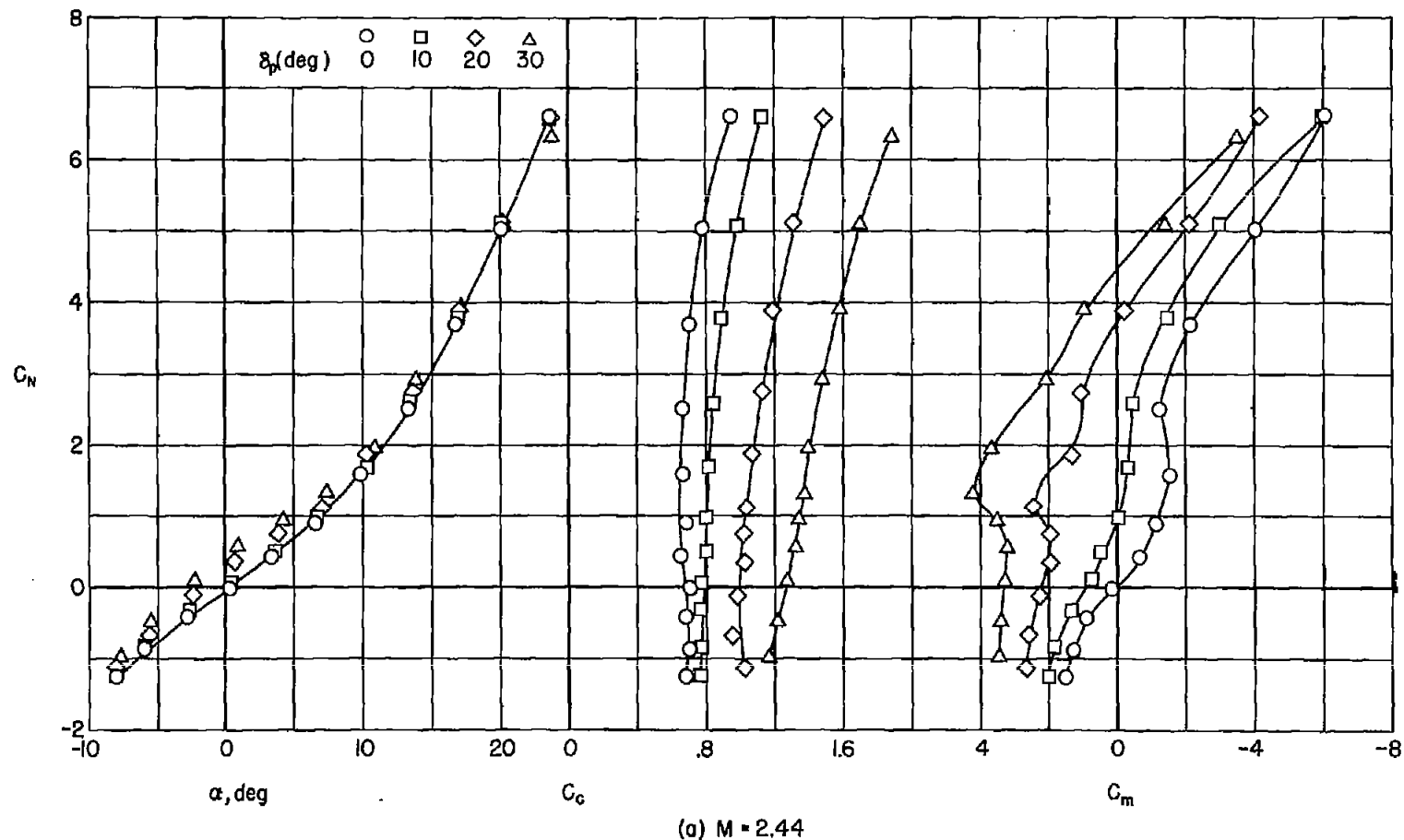
(a) $M = 2.44$

Figure 2.- Aerodynamic characteristics of wingless missile.

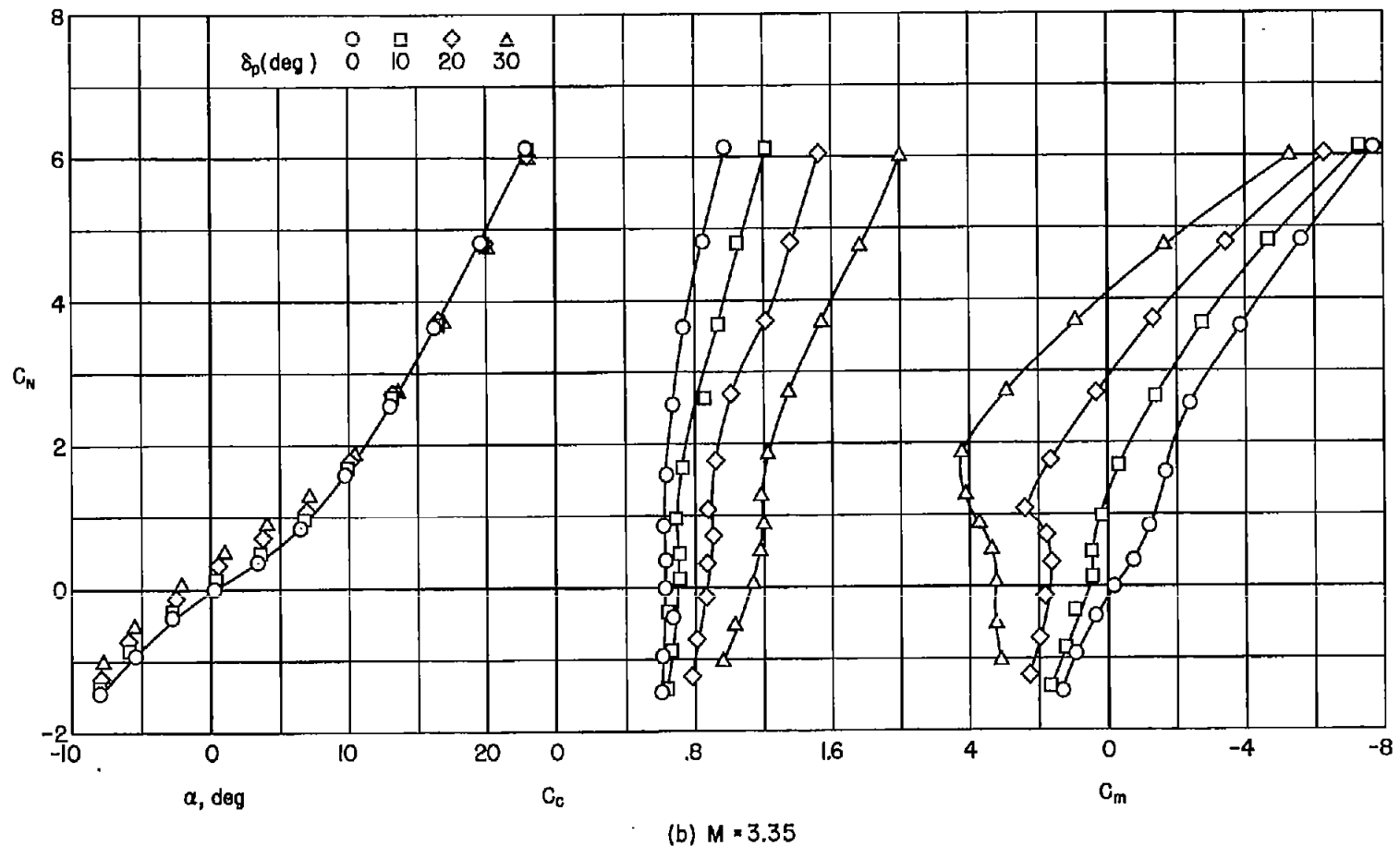
(b) $M = 3.35$

Figure 2.- Concluded.

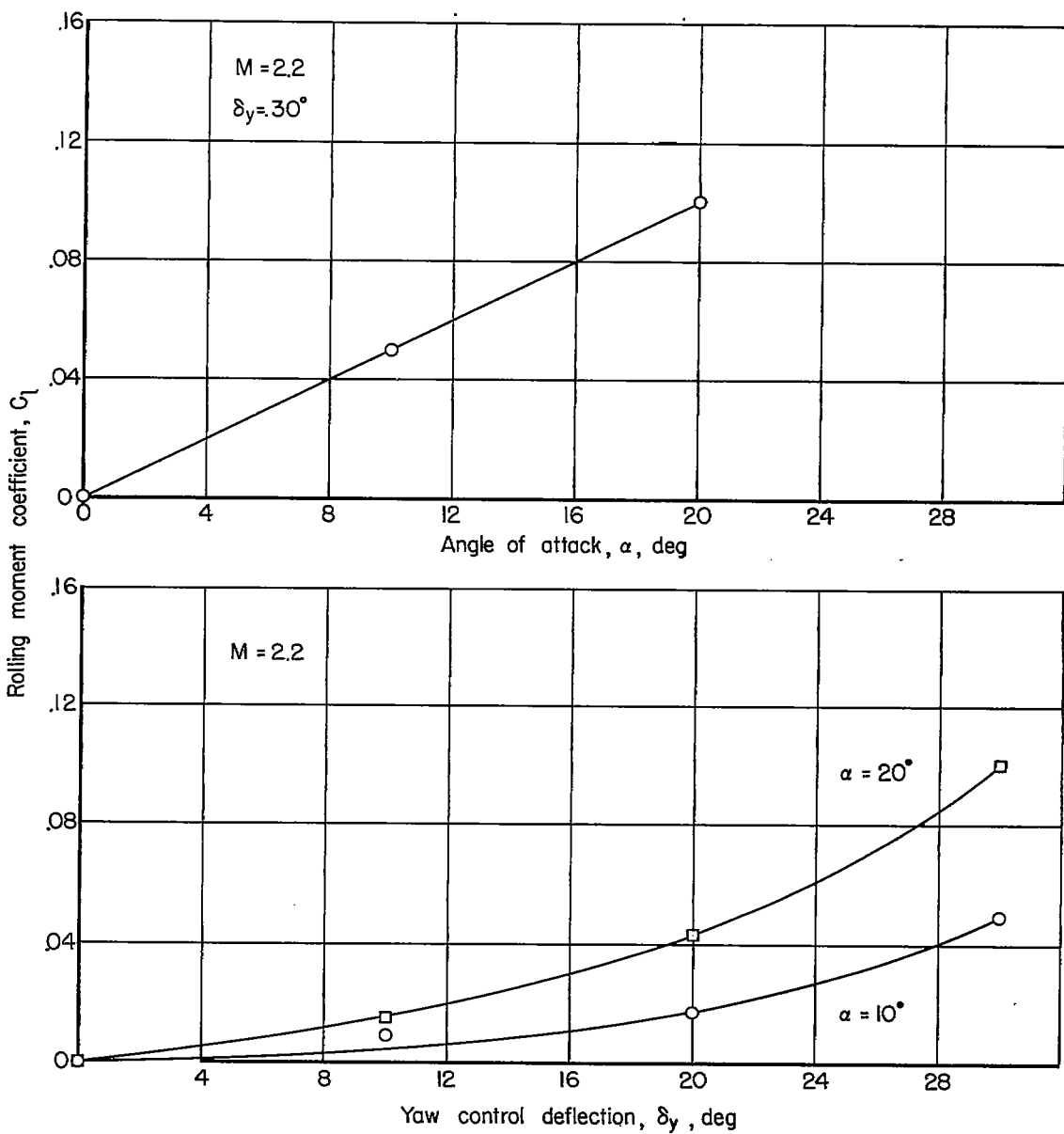


Figure 3.- Variation of rolling moment with angle of attack and control deflection - tail off.

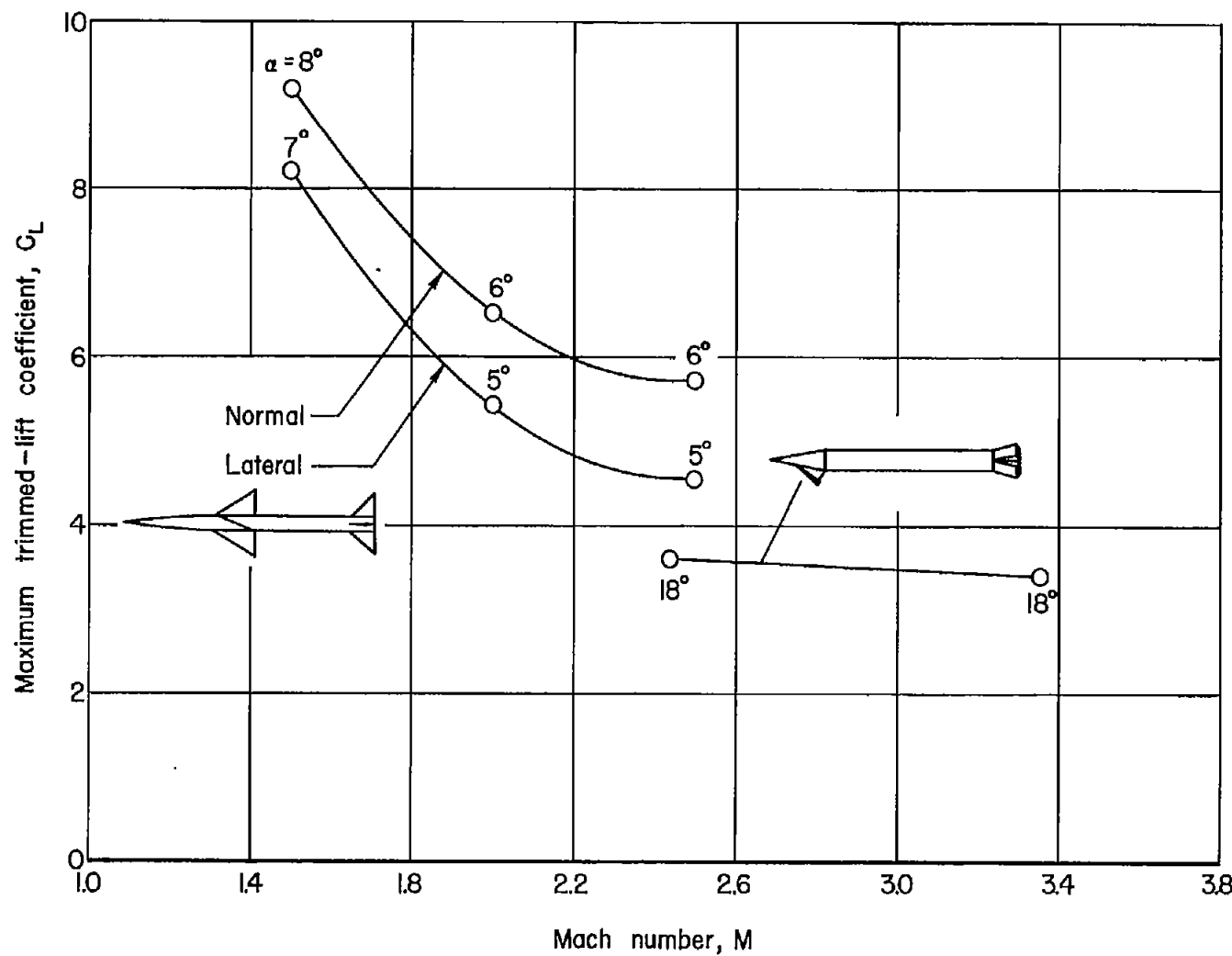


Figure 4.- The maximum trimmed-lift coefficients of the cruciform and wingless missiles.

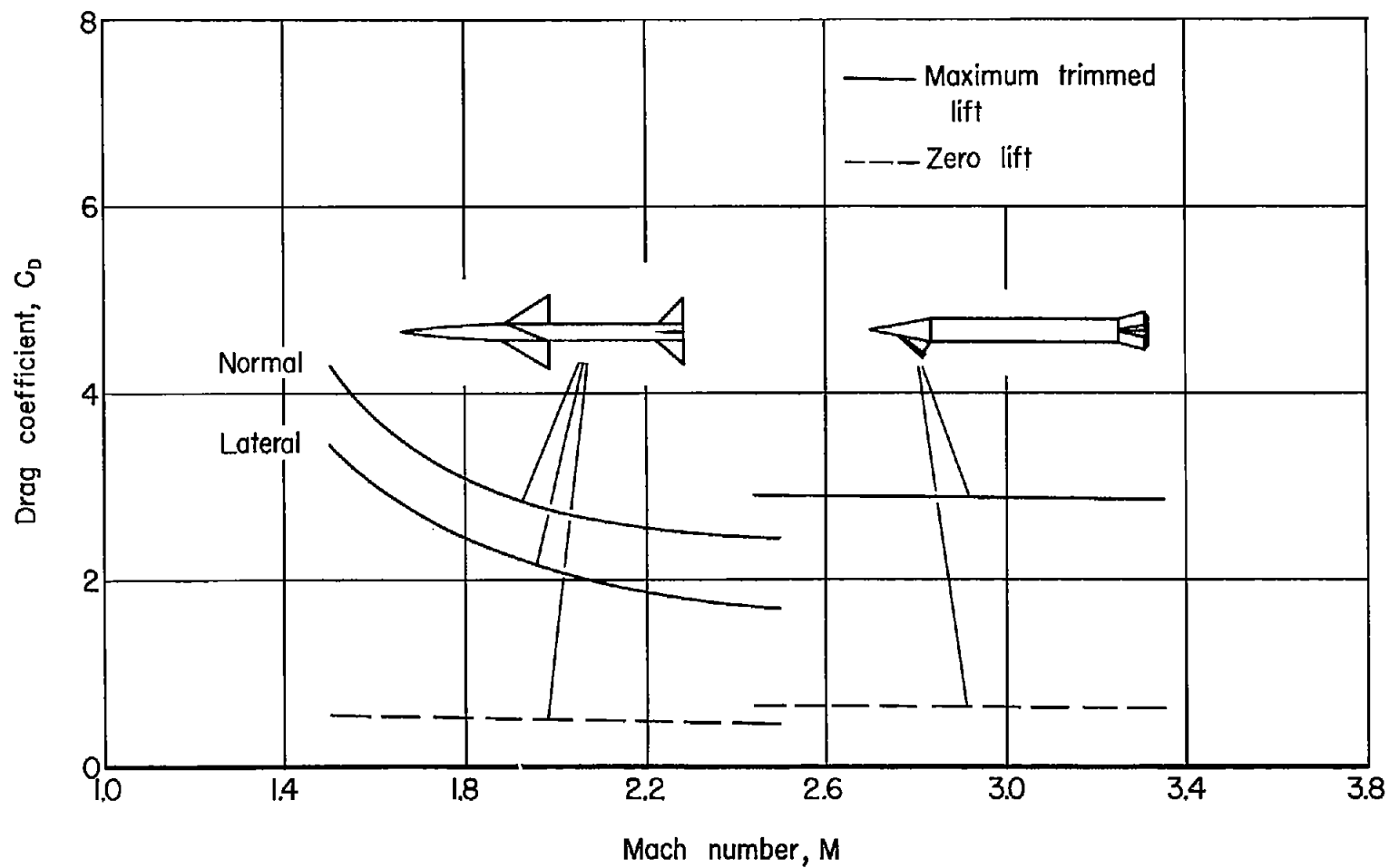


Figure 5.- Comparison of the zero-lift and maneuvering drag coefficient for the cruciform and wingless configuration.

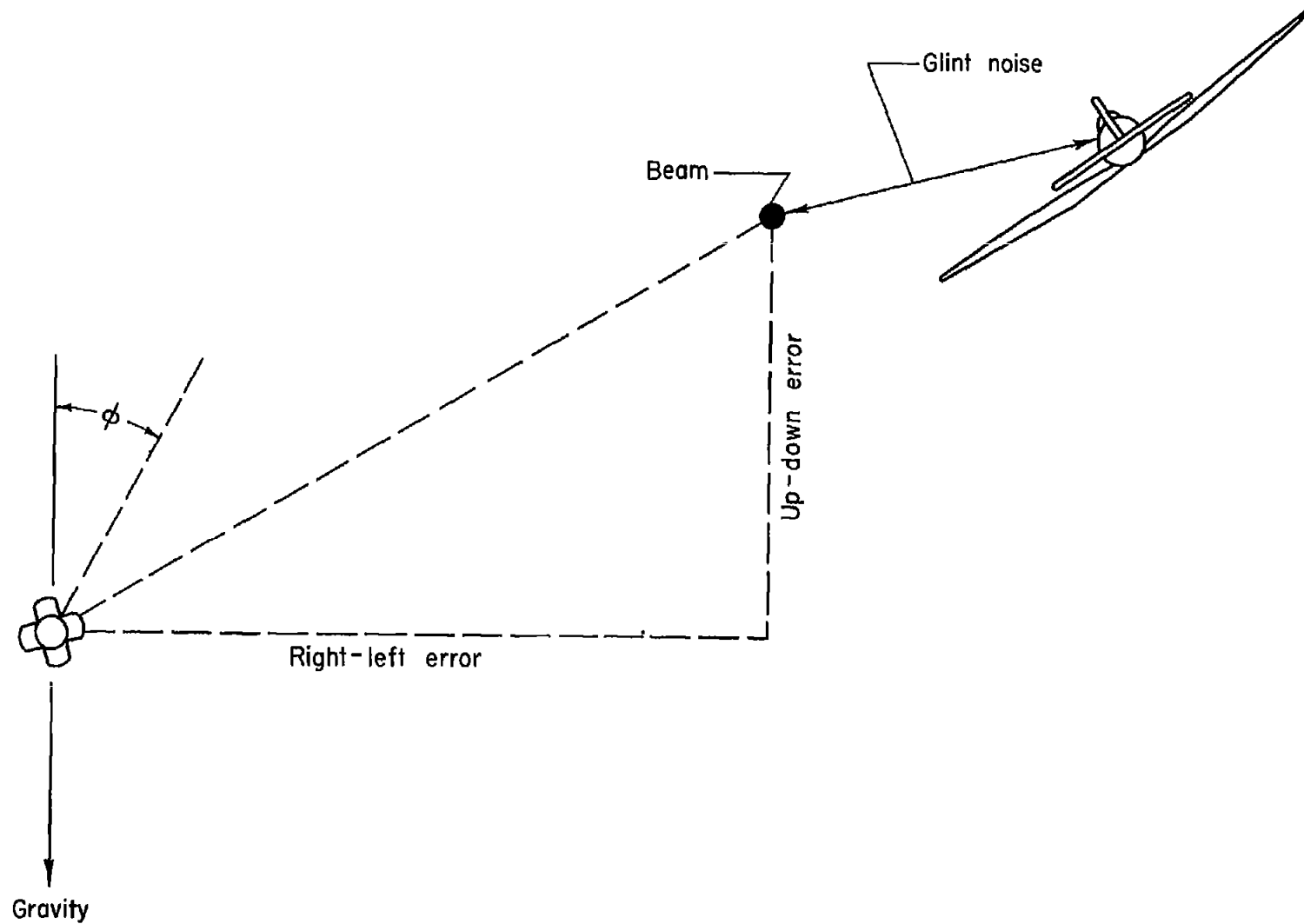


Figure 6.- Beam-rider geometry.

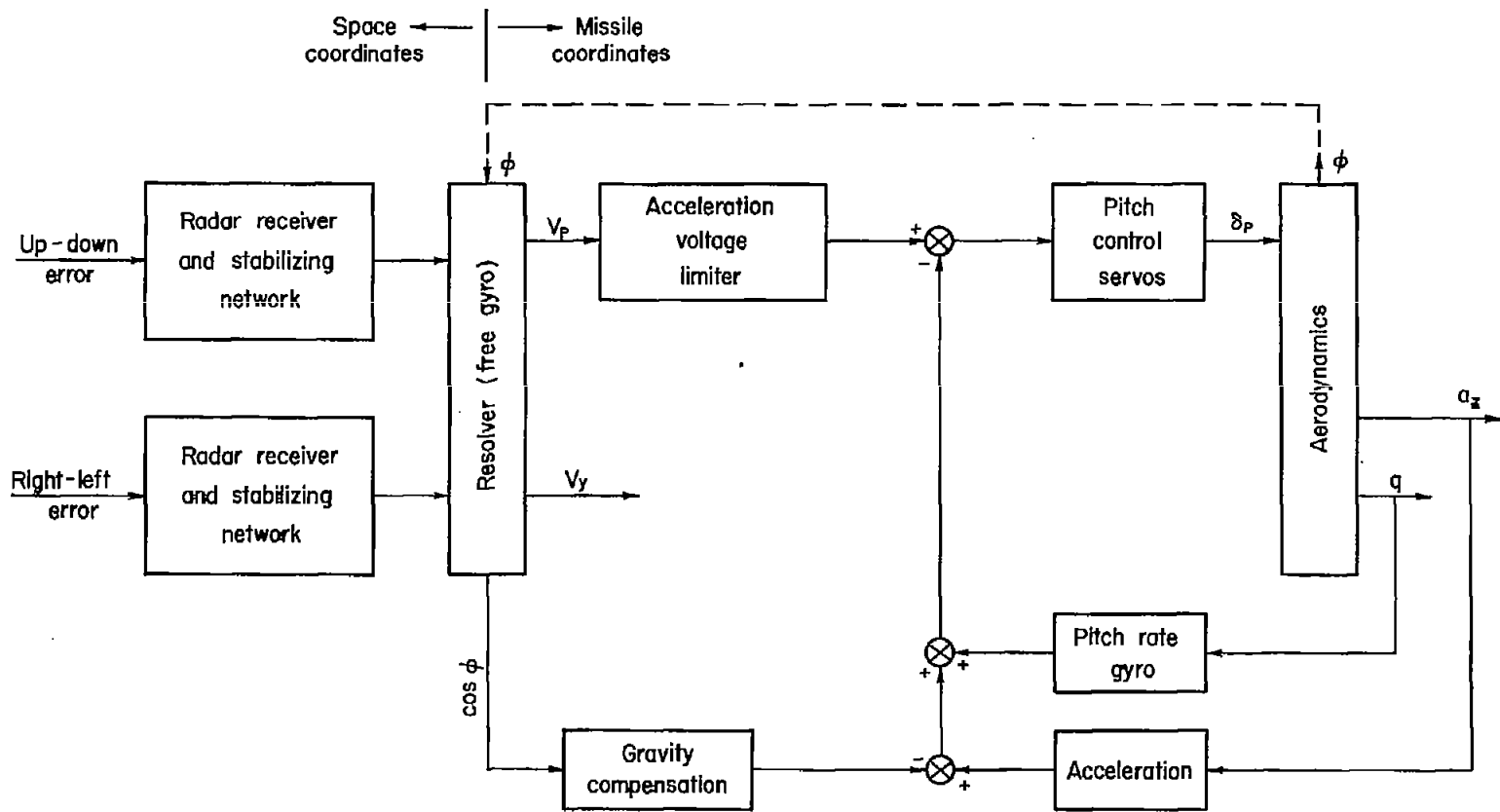


Figure 7.—Block diagram of control system.

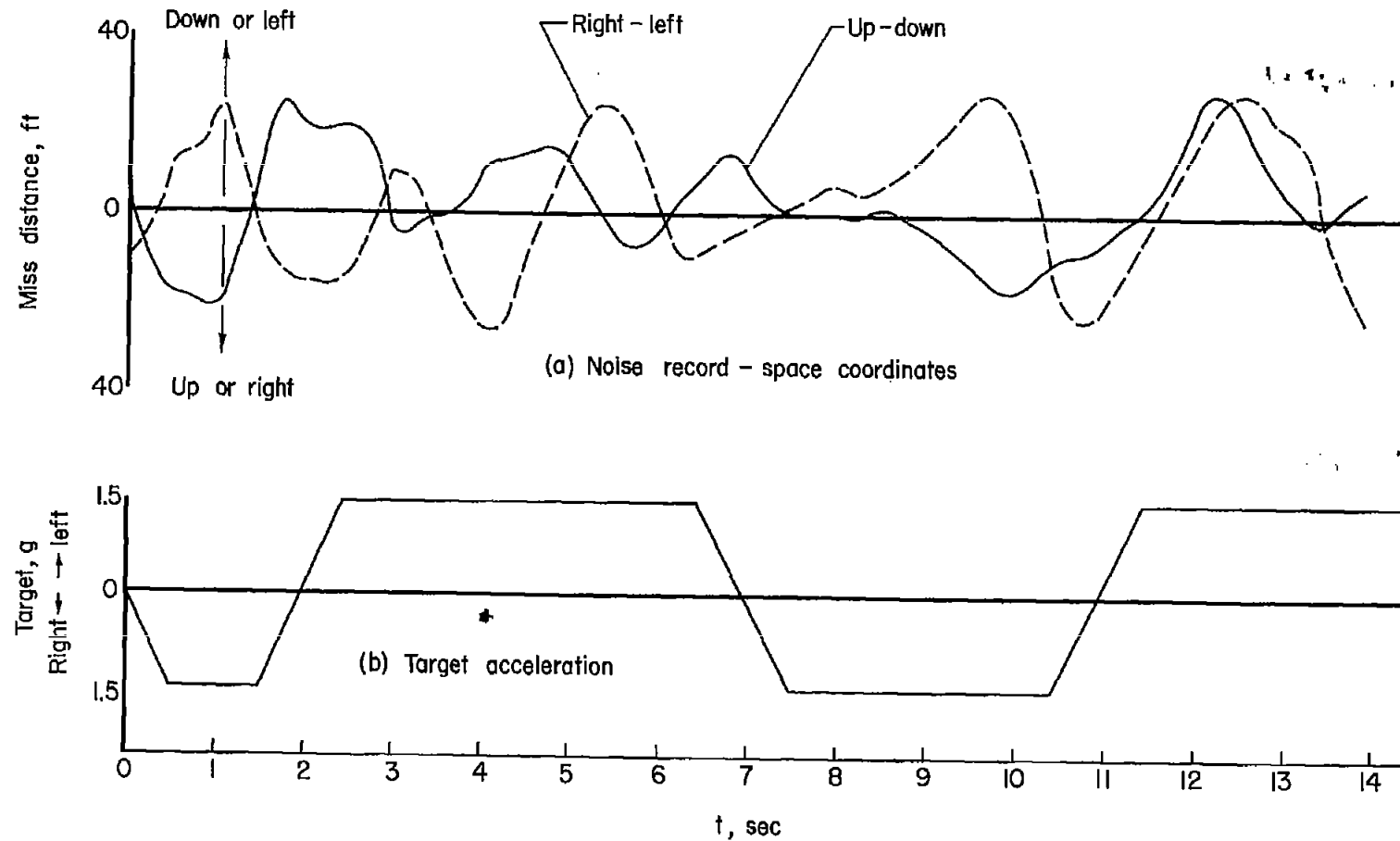


Figure 8.— Beam inputs.

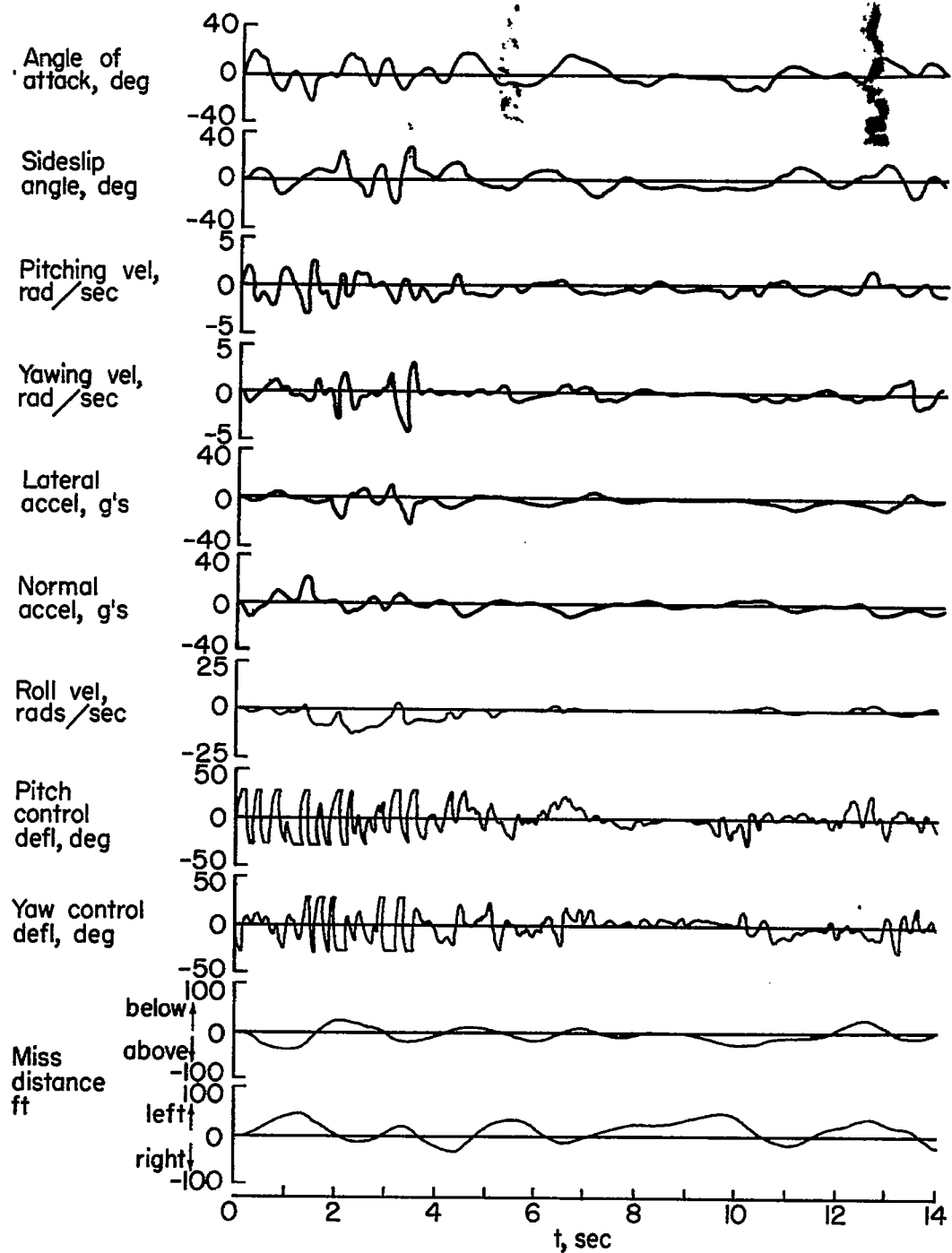


Figure 9. - Tracking results for wingless missile; $M = 3.35$, altitude = 50,000 ft.